BCSIR

Avaiable online at www.babglajol.info

Bangladesh J. Sci. Ind. Res. **43(2)**, 159-172, 2008

BANGLADESH JOURNAL OF SCIENTIFIC AND INDUSTRIAL RESEARCH

E-mail: bjsir07gmail.com

Dufour and Soret Effects on Unsteady MHD Free Convection and Mass Transfer Fluid Flow Through a Porous Medium in a Rotating System

Nazmul Islam and Md. Mahmud Alam*

Mathematics Discipline, Khulna University, Khulna-9208, Bangladesh

Abstract

The numerical studies are performed to examine the unsteady MHD free convection and mass transfer flow through a porous medium with thermal diffusion and diffusion thermo past an infinite vertical porous plate in a rotating system. Method of superposition is used as a main tool for numerical solution. The study is mainly based on the similarity approach. Impulsively started plate moving in its own plane is considered. Similarity equations of the corresponding momentum, energy and concentration equations are derived by introducing a time dependent length scale which infact plays the role of a similarity parameter. The velocity component is taken to be inversely proportional to this parameter. The effects on the velocity, temperature, concentration, local skin-friction coefficients, Nusselt number and the Sherwood number of the various important parameters entering into the problem separately are discussed with the help of graphs and tables.

Key words : Numerical studies, Magnetohydronamics, Dufour, Soret, Rotating system

Nomenclature

x, y, z,	Cartesian coordinates
t	Time
u, v, w	Fluid velocities
v_0	Velocity of suction
μ	Kinematics viscosity
η	Similarity variables
υ	Coefficient of kinematics viscosity
θ	Dimensionless temperature
φ	Dimensionless concentration
ρ	Fluid density
$\mathbf{B}$	Magnetic field
β	Coefficient of volume expansion
β^*	Volumetric coefficient of expansion with concentration
g_0	Acceleration due to gravity
U_0	Uniform velocity
T	Temperature
T_w	Plate temperature
T_∞	Free stream temperature
C	Concentration

* Corresponding author

C_w Plate concentration
C_∞ Free stream concentration
G_r Grashof number
G_m Modified grashof number
K Permeability parameter
C_w Plate concentration
C_∞ Free stream concentration
G_r Grashof number
G_m Modified grashof number
K Permeability parameter
P_r Prandtl number
S_c Schimidt number
S_r Soret number
D_f Dufour number
M Magnetic prameter
R Rotation parameter
K Permeability of the porous medium
D_m Coefficient of mass diffusivity
c_p Specific heat at constant pressure
T_m Mean fluid temperature
k_T Thermal diffusion ratio
c_s Concentration susceptibility

Introduction

The science of magnetohydrodynamics (MHD) was concerned with geophysical and astrophysical problems for a number of years. In recent years the possible use of MHD is to affect a flow stream of an electrically conducting fluid for the purpose of thermal protection, braking, propulsion and control. From the point of applications, model studies on the effect of magnetic field on free convection flows have been made by several investigators. Some of them are Georgantopoulos (1979), Nanousis *et al.* (1980) and Raptis and Singh (1983). Along with the effects of magnetic field, the effect of transpiration parameter, being an effective method of controlling the boundary layer has been considered by Singh (1982). On the other hand, along with the free convection currents, caused by the temperature difference, the flow is also effected by the difference in concentrations on material constitution. Gebhart and Pera (1971) made extensive studies of such a combined heat and mass transfer flow to highlight the insight of the flow.

In the above mentioned works, the level of concentration of foreign mass is assumed very low so that the Soret and Dufour effects are neglected. However, exceptions are observed therein. The Soret effect, for instance, has been utilized for isotope separation, and in mixture between gases with very light molecular weight (H_2, H_e) and of medium molecular weight (N_2,, air). The Dufour effect was found to be of order of considerable magnitude such that it cannot be ignored (Eckert and Drake, 1972). In view of the importance of above mentioned effects, Kafoussias and Williams (1995) studied the Soret and Dufour effects on mixed free-forced convective and mass transfer boundary layer flow with temperature dependent viscosity. Anghel *et al.* (2000) investigated the Dufour and Soret effects on free convection boundary layer flow over a vertical surface embedded in a porous medium. Quite recently, Alam and Rahman (2006) investigated the Dufour and Soret effects on mixed convection flow past a vertical porous flat plate with variable suction.

In consequence of the above studies, several investigators disclosed that the Coriolis force is very significant as compared to viscous and inertia forces occurring in the basic fluid equations. It is generally admitted that the Coriolis force due to Earth's rotation has a strong effect on the hydromagnetic flow in the Earth's liquid core. The study of such fluid flow problem is important due to its applications in various branches of geophysics, astrophysics and fluid engineering. From the point of application in solar physics and cosmic fluid dynamics, it is important to consider the effects of the electromagnetic and rotation forces on the flow. Considering this aspect of the rotational flows, model studies were carried out on MHD free convection and mass transfer flows in a rotating system by many investigators of whom the names are Debnath (1975), Debnath *et al*. (1979) and Raptis and Perdikis (1982) are worth mentioning. Singh (1984), Raptis and Singh (1985) and Singh and Singh (1989) have made a few studies by taking various aspects of the flow phenomena. But no works of the simultaneous effects of the electromagnetic and rotation forces on the hydromagnetic free convection and mass transfer with Dufour and Soret effects have been reported in the literature.

Hence, our objective is to investigate the Dufour and Soret effects on unsteady MHD free convection and mass transfer flow through a porous medium past an infinite vertical porous plate in a rotating system.

Governing Equation

Consider an unsteady MHD free convection and mass transfer flow of an electrically conducting viscous fluid through a porous medium along an infinite vertical porous plate y=0 in a rotating system. The flow is also assumed to be in the x-direction which is taken along the plate in the upward direction and y -axis is normal to it. Initially the fluid as well as the plate is at rest, after that the whole system is allowed to rotate with a constant angular velocity Ω about the y -axis. The temperature and the species concentration at the plate are constantly raised from T_w and C_w to T_∞ and C_∞ respectively, which are thereafter maintained constant, where T_∞ and C_∞ are the temperature and species concentration of the uniform flow respectively. A uniform magnetic field **B** is taken to be acting along the *y-axis* which is assumed to be electrically non-conducting. We assumed that the magnetic Reynolds number of the flow is taken to be small enough so that the induced magnetic field is negligible in comparison with applied one (Pai, 1962), so that $\mathbf{B}=(0,B_0,0)$ and the magnetic lines of force are fixed relative to the fluid. The equation of conservation of charge $\nabla.\mathbf{J}=0$ gives J_y= constant, where the current density $\mathbf{J}=(J_x, J_y, J_z)$. Since the plate is electrically non-conducting, this constant is zero and hence J_y = 0 at the plate and hence zero everywhere.

The physical configuration considered here is shown in the following Fig. 1.

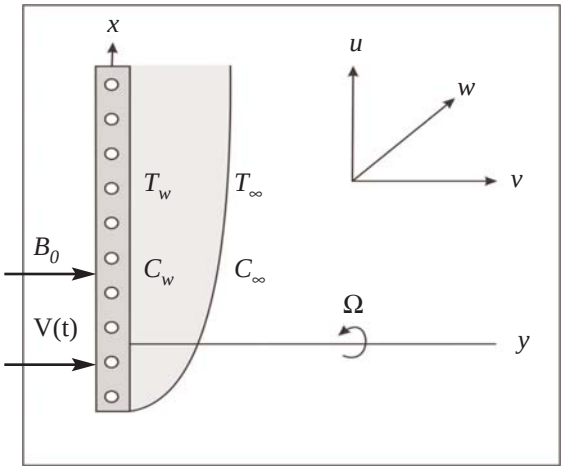

Fig. 1. Physical configuration and coordinate system

With in the frame of such assumptions, neglecting the Joule heating and viscous dissipation terms and under the usual Boussineq's approximation, the governing equations relevant to the problem are

The continuity equation:

$$\frac{\partial v}{\partial y} = 0 \tag{1}$$

The momentum equations:

$$\frac{\partial u}{\partial t} + v\frac{\partial u}{\partial y} = g_0\beta\left(T - T_\infty\right) + g_0\beta^*\left(C - C_\infty\right)$$

$$+\upsilon\frac{\partial^2 u}{\partial y^2} + 2\Omega w - \frac{\upsilon}{K'}u - \frac{\sigma' B_0{}^2 u}{\rho} \tag{2}$$

$$\frac{\partial w}{\partial t} + v\frac{\partial w}{\partial y} = \upsilon\frac{\partial^2 w}{\partial y^2} - 2\Omega u - \frac{\upsilon}{K'}w - \frac{\sigma' B_0{}^2 w}{\rho} \tag{3}$$

The energy equation:

$$\frac{\partial T}{\partial t} + v\frac{\partial T}{\partial y} = \frac{k}{\rho c_p}\frac{\partial^2 T}{\partial y^2} + \frac{D_m k_T}{c_s c_p}\frac{\partial^2 C}{\partial y^2} \tag{4}$$

The concentration equation:

$$\frac{\partial C}{\partial t} + v\frac{\partial C}{\partial y} = D_m\frac{\partial^2 C}{\partial y^2} + \frac{D_m k_T}{T_m}\frac{\partial^2 T}{\partial y^2} \tag{5}$$

where all physical quantities are defined in the nomenclature.

The boundary conditions for the present problem are

$$t \le 0, u = 0, v = 0, w = 0, T = T_\infty, C = C_\infty$$

for all values of y

$$\left.\begin{aligned} t > 0, u = U_0, v = v(t), w = 0, T = T_w, C = C_w \text{ at } y = 0 \\ t > 0, u = 0, v = 0, w = 0, T \to T_\infty, C \to C_\infty \text{ at } y \to \infty \end{aligned}\right\} \tag{6}$$

In order to obtain similar solutions we introduce a similarity parameter σ as

$$\sigma = \sigma(t) \tag{7}$$

such that σ is the time dependent length scale. In terms of this length scale, a convenient solution of equation (1) is considered to be

$$v = -v_0\frac{\upsilon}{\sigma}\,. \tag{8}$$

Here the constant v_0 represents a dimensionless normal velocity at the plate which is positive for suction and negative for blowing.

We now introduce the following dimensionless variables to attain a similarity solution

$$\left.\begin{aligned} \eta &= \frac{y}{\sigma} \\ f(\eta) &= \frac{u}{U_0} \\ g(\eta) &= \frac{w}{U_0} \\ \theta(\eta) &= \frac{T - T_\infty}{T_w - T_\infty} \\ \phi(\eta) &= \frac{C - C_\infty}{C_w - C_\infty} \end{aligned}\right\} \quad (9)$$

Then introducing equations (8)-(9) into equations (2)-(5), we obtain

$$-\frac{\sigma}{\upsilon}\frac{\partial\sigma}{\partial t}\eta f' - v_0 f' = f'' + G_r\theta + G_m\phi - Kf - Mf - 2Rg \quad (10)$$

$$-\frac{\sigma}{\upsilon}\frac{\partial\sigma}{\partial t}\eta g' - v_0 g' = g'' - Kg - Mg + 2Rf \quad (11)$$

$$\theta \qquad -\frac{\sigma}{\upsilon}\frac{\partial\sigma}{\partial t}\eta\vartheta' - v_0\theta' = \frac{1}{P_r}\theta'' + D_f\phi'' \quad (12)$$

$$-\frac{\sigma}{\upsilon}\frac{\partial\sigma}{\partial t}\eta\phi' - v_0\phi' = \frac{1}{S_c}\phi'' + S_r\theta'' \quad (13)$$

where $G_r = \dfrac{g_0\beta(T_w - T_\infty)\sigma^2}{U_0\upsilon}$,

$G_m = \dfrac{g_0\beta^*(C_w - C_\infty)\sigma^2}{U_0\upsilon}$,

$M = \dfrac{\sigma' B_0{}^2\sigma^2}{\rho\upsilon}$,

$R = \dfrac{\Omega\sigma^2}{\upsilon}$, $P_r = \dfrac{\rho\upsilon c_p}{k}$,

$D_f = \dfrac{D_m k_T}{c_s c_p \upsilon}\dfrac{(C_w - C_\infty)}{(T_w - T_\infty)}$, $S_c = \dfrac{\upsilon}{D_m}$ and

$S_r = \dfrac{D_m k_T}{\upsilon T_m}\dfrac{(T_w - T_\infty)}{(C_w - C_\infty)}$ and where all physical quantities are defined in the nomenclature.

The equations (10)-(13) are similar except for the term $\dfrac{\sigma}{\upsilon}\dfrac{\partial\sigma}{\partial t}$ where time t appears explicitly. Thus the similarity condition requires that $\dfrac{\sigma}{\upsilon}\dfrac{\partial\sigma}{\partial t}$ in the equations (10)-(13) must be a constant quantity. Hence following the works of Sattar and Alam (1994) one can try a class of solutions of the equations (10)-(13) by assuming that

$$\frac{\sigma}{\upsilon}\frac{\partial\sigma}{\partial t} = c \text{ (a constant)} \quad (14)$$

Now integrating (14) one obtains

$$\sigma = \sqrt{2c\upsilon t} \quad (15)$$

where the constant of integration is determined through the condition that σ = 0 when t=0. It thus appears from (15) that, by making a realistic choice of c to be equal to 2 in (14) the length scale σ becomes equal to $\sigma = 2\sqrt{\upsilon t}$ which exactly corresponds to the usual scaling factor considered for various

unsteady boundary layer flows (Schlichting, 1968). Since σ is a scaling factor as well as a similarity parameter, any other value of c in (14) would not change the nature of the solution except that the scale would be different. Finally, introducing (14) with $c = 2$ in equations (10)-(13), we respectively have the following dimensionless ordinary differential equations

$$f'' + 2\xi f' + G_r\theta + G_m\phi - Kf - Mf - 2Rg = 0 \quad (16)$$

$$g'' + 2\xi g' - Kg - Mg + 2Rf = 0 \quad (17)$$

$$\theta'' + 2\xi P_r\theta' + P_r D_f \phi'' = 0 \quad (18)$$

$$\phi'' + 2\xi S_c\phi' + S_c S_r\theta'' = 0 \quad (19)$$

where $\xi = \eta + \frac{v_0}{2}$.

The corresponding boundary conditions are

$$\left.\begin{array}{l} f = 1,\ g = 0,\ \theta = 1,\ \phi = 1 \quad at \quad \eta = 0 \\ f = 0,\ g = 0,\ \theta = 0,\ \phi = 0 \quad as \quad \eta \to \infty \end{array}\right\} \quad (20)$$

In all the above equations primes denote the differentiation with respect to η.

Solutions

The solutions of equations (16)-(19) are now obtained by the method of superposition (Na, 1979). The essence of this method is to reduce the boundary value problem to an initial value problem which can easily be integrated out, without any iteration, by any initial value solver.

For the purpose of numerical integration, the well known Runge-Kutta Merson Integration Scheme has been used as an initial value problem solver to integrate the above mentioned equations and to obtain converged solutions. If now τ_x, τ_z, N_u and S_h respectively denote the local values of the x and z components of the skin-friction, the Nusselt number and the Sherwood number they are respectively proportional to $\frac{\partial f(0)}{\partial \eta}$, $\frac{\partial g(0)}{\partial \eta}$, $-\frac{\partial \theta(0)}{\partial \eta}$ and $-\frac{\partial \varphi(0)}{\partial \eta}$. ϕ

The numerical values of local skin-friction coefficients, the Nusselt number and the Sherwood number are sorted in Tables I-III.

Results and Discussion

The velocity profiles for x and z components of velocity, commonly known as non-dimensional primary (f) and secondary (g) velocities, are shown in Figs. 2 - 17 for different values of suction parameter (v_0), the magnetic parameter (M), the rotation parameter (R), the Prandtl number (P_r), the Soret number (S_r), the Schmidt number (S_c), the Dufour number (D_f) and the permeability parameter (K) and for fixed values of Grashof number (G_r) and modified Grashof number (G_m). The values of Grashof number (G_r) and modified Grashof number (G_m) are taken to be large, since these value correspond to a cooling problem that is generally encountered in nuclear engineering in connection with the cooling of reactors. For Prandtl number (P_r), three values 0.71, 1.0 and 7.0 are considered (0.71 represents air at

20^0 C, 1.0 corresponds to electrolyte solutions such as salt water and 7.0 correspond to water). The values 0.22, 0.60 and 0.75 of the Schmidt number (S_c) are also considered for they represent specific conditions of the flow. In particular, 0.22 corresponds to hydrogen while 0.60 corresponds to water vapor that represents a diffusivity chemical species of most common interest in air and the value 0.75, represent oxygen. The values of v_o , M, R, S_r, D_f, K and G_m are however chosen arbitrary.

Table I. Numerical values of τ_x, τ_z, N_u and S_h for P_r = 0.71, G_r=10.0, G_m = 4.0, R=0.2, S_r , = 1.0, S_c = 0.6, D_f = 0.2 and K=0.5

v_0	M	τ_x	τ_z	N_u	S_h
0.5	0.5	2.7611793	-1.2612417	1.3540955	0.7810146
1.0	0.5	2.3337250	-1.1613957	1.5962112	0.8407938
1.5	0.5	1.8513867	-1.0594143	1.8520351	0.9010674
0.5	1.0	2.4824549	-1.1592220	1.3540893	0.7810245
0.5	1.5	2.2226458	-1.0718636	1.3540834	0.7810350

Table II. Numerical values of τ_x, τ_z, N_u and S_h for v_0 = 0.5, G_r=10.0, G_m = 4.0, M=0.5, P_r = 0.71, S_c = 0.6, D_f = 0.2 and K=0.5

R	S_r	τ_x	τ_z	N_u	S_h
0.2	1.0	2.9867173	-0.2631226	1.3539250	0.7808163
0.4	1.0	2.9565132	-0.5232471	1.3540188	0.7809357
0.6	1.0	2.9080943	-0.7778524	1.3540590	0.7809765
0.2	2.0	3.0757815	-1.4052470	1.3790387	0.5116685
0.2	3.0	3.2797583	-1.4241212	1.4983555	-0.4302568

Table III. Numerical values of τ_x, τ_z, N_u and S_h for v_0 = 0.5, G_r=10.0, G_m = 4.0, P_r = 0.71, R=0.2, M=0.5, S_r = 1.0, and S_c = 0.6

D_f	K	τ_x	τ_z	N_u	S_h
0.2	0.5	2.7611793	-1.2612417	1.3540955	0.7810146
0.5	0.5	2.9102812	-1.3154989	1.2759578	0.8169440
0.8	0.5	3.0681069	-1.3706838	1.1795134	0.8630274
0.2	1.0	2.4824549	-1.1592220	1.3540893	0.7810245
0.2	1.5	2.2226458	-1.0718636	1.3540834	0.7810350

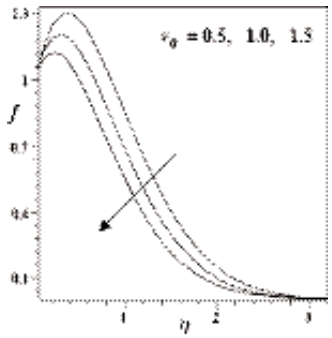

Fig. 2. Primary velocity profiles for different values of v_o with G_r=10.0, G_m =4.0, M=0.5, R=0.2, P_r= 0.71, S_r= 1.0, S_c= 0.6, D_f= 0.2, K= 0.5.

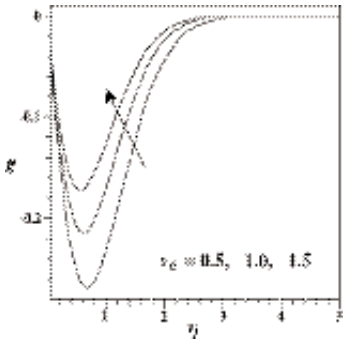

Fig. 3. Secondary velocity profiles for different values of v_o with G_r=10.0, G_m =4.0, M=0.5, R=0.2, P_r= 0.71, S_r= 1.0, S_c= 0.6, D_f= 0.2, K= 0.5.

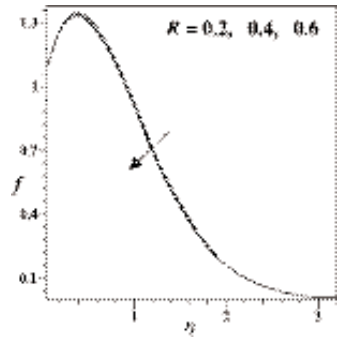

Fig. 4. Primary velocity profiles for different values of R with v_o=0.5, G_r=10.0, G_m =4.0, M=0.5, P_r= 0.71, S_r= 1.0, S_c= 0.6, D_f= 0.2, K= 0.5.

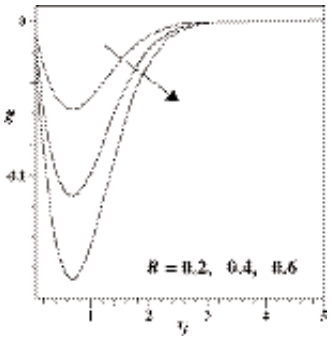

Fig. 5. Secondary velocity profiles for different values of R with v_o=0.5, G_r=10.0, G_m =4.0, M=0.5, P_r= 0.71, S_r= 1.0, S_c= 0.6, D_f= 0.2, K= 0.5.

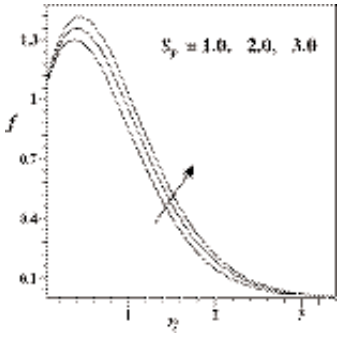

Fig. 6. Primary velocity profiles for different values of S_r with v_o=0.5,G_r=10.0, G_m=4.0, M=0.5, R=0.2, P_r= 0.71, S_c= 0.6, D_f= 0.2, K= 0.5.

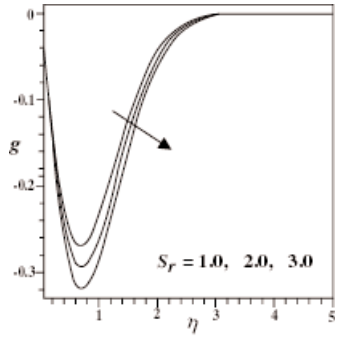

Fig. 7. Sceondary velocity profiles for different values of S_r with v_o=0.5, G_r=10.0, G_m =4.0, M=0.5, R=0.2, P_r= 0.71, S_c= 0.6, D_f= 0.2, K= 0.5.

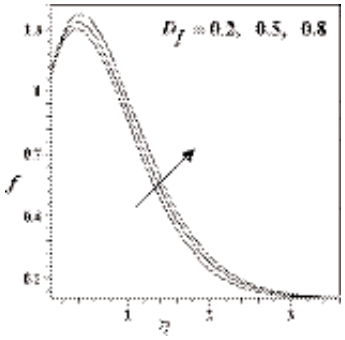

Fig. 8. Primary velocity profiles for different values of D_f with v_o=0.5, G_r=10.0, G_m =4.0, M=0.5, R=0.2, P_r= 0.71, S_r= 1.0, S_c= 0.6, K= 0.5.

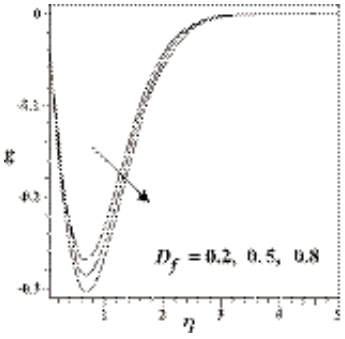

Fig. 9. Secondary velocity profiles for different values of D_f with v_o=0.5, G_r=10.0, G_m =4.0, M=0.5, P_r= 0.71, S_r= 1.0, S_c= 0.6, K= 0.5.

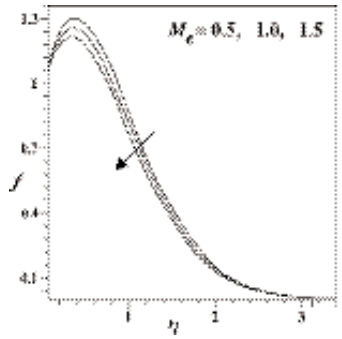

Fig. 10. Primary velocity profiles for different values of M with v_o=0.5, G_r=10.0, G_m =4.0, R=0.2, P_r= 0.71, S_r= 1.0, S_c= 0.6, D_f= 0.2, K= 0.5.

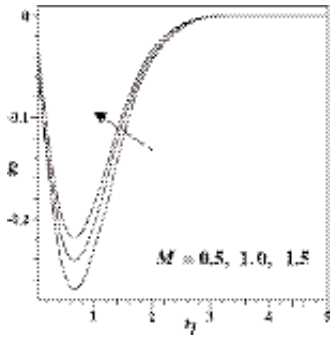

Fig. 11. Secondary velocity profiles for different values of M with v_o=0.5, G_r=10.0, G_m =4.0, R=0.2, P_r= 0.71, S_r= 1.0, S_c= 0.6, D_f= 0.2, K= 0.5.

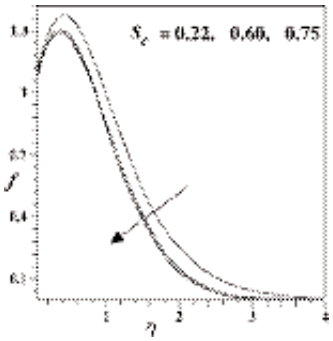

Fig. 12. Primary velocity profiles for different values of S_c with v_o=0.5,G_r=10.0, G_m=4.0, M=0.5, R=0.2, P_r= 0.71, S_r= 1.0, D_f= 0.2, K= 0.5.

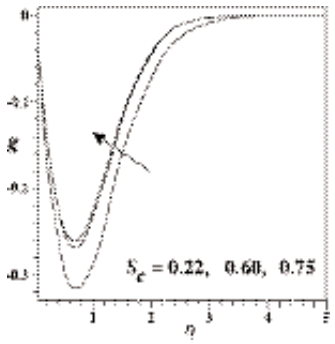

Fig. 13. Secondary velocity profiles for different values of S_c with v_o=0.5, G_r=10.0, G_m =4.0, M=0.5, R=0.2, P_r= 0.71, S_r= 1.0, D_f= 0.2, K= 0.5.

With the above mentioned parameters, the velocity profiles for the primary and the secondary velocities are presented in Figs. 2 - 17, the temperature profiles are presented in Figs. 18 - 20 and the concentration profiles are presented in Figs. 21 -24.

The effects of the suction parameter (v_o) on the primary and secondary velocities are shown in Figs. 2 and 3. It is observed from these figures that an increase in the suction parameter (v_o) leads, respectively, to a decrease in the primary velocity and to an increase in the secondary velocity. The usual stabilizing effect of the suction parameter on the boundary layer growth is also evident from these figures.

In Figs. 4 and 5, the effects of rotation parameter (R) on the primary and secondary velocities are shown respectively. It is observed from these figures that the rotation parameter has minor decreasing effect on the primary velocity while the same has quite larger decreasing effect on the secondary velocity. In Figs. 6 and 7 and 8 and 9, the effects of Soret number (S_r) and Dufour number (D_f) on the primary and secondary velocities are shown respectively. It is observed from these figures that the primary velocity increases while the secondary velocity decreases with the increase of Soret number (S_r). The same effect is observed from these figures in case of Dufour number (D_f). The effects of magnetic parameter (M), Schmidt number (S_c), permeability parameter (K) and Prandtl number (P_r) on the primary and secondary velocities are shown respectively in Figs. 10 and 11, 12 and 13, 14 and 15, and 16 and 17. From Figs. 10 and 11, it is observed that the primary velocity decreases while the secondary velocity increases with the increase of magnetic parameter (M). The same effects are observed from Figs. 12 and 13 and 14 and 15 in case of Schmidt number (S_c) and permeability parameter (K) respectively. From Figs. 16 and 17, it is seen that the Prandtl number (P_r) has quite a larger decreasing effect on the primary velocity while it has a similar increasing effect on the secondary velocity.

The effects of suction parameter (v_o) on the temperature field is shown in Fig. 18. It is observed from this figure that the temperature decreases as the suction parameter (v_o) increase. In Fig. 19, the effects of Dufour number (D_f) on the temperature field is shown. It is observed from this figure that the temperature increases as the Dufour number (D_f) increase.

In Fig. 20, the effects of Prandtl number (P_r) on the temperature field is shown. It is observed from this figure that as the Prandtl number increases the temperature decrease at a particular position of the boundary layer. This decrease is very large in case of water (P_r=7.0). We also observe that for P_r=7.0 the field temperature remains less than the uniform flow temperature for most part of the boundary layer.

The effects of suction parameter (v_o) on the concentration field are displayed in Fig. 21, which shows that the concentration decreases as the suction parameter (v_o) increase. In Fig. 22, the effect of Soret number (S_r) on the concentration field is displayed. It is

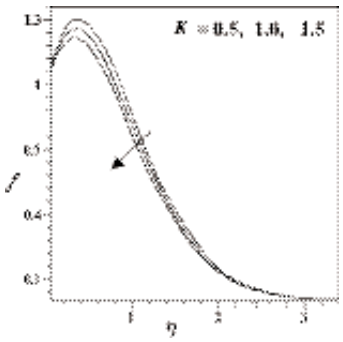

Fig. 14. Primary velocity profiles for different values of K with v_o=0.5, G_r=10.0, G_m =4.0, M=0.5, R=0.2, P_r= 0.71, S_r= 1.0, S_c= 0.6, D_f= 0.2.

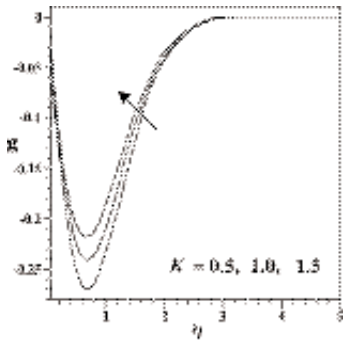

Fig. 15. Secondary velocity profiles for different values of K with v_o=0.5, G_r=10.0, G_m =4.0, M=0.5, R=0.2, P_r= 0.71, S_r= 1.0, S_c= 0.6, D_f= 0.2,.

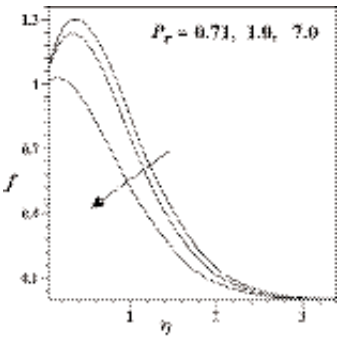

Fig. 16. Primary velocity profiles for different values of P_r with v_o=0.5, G_r=10.0, G_m =4.0, M=0.5, R=0.2, S_r= 1.0, S_c= 0.6, D_f= 0.2, K= 0.5.

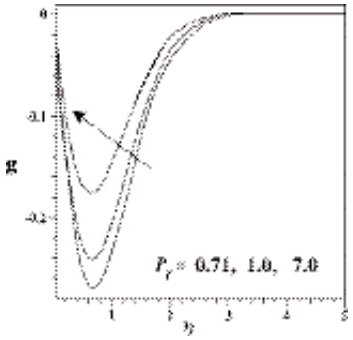

Fig. 17. Secondary velocity profiles for different values of P_r with v_o=0.5, G_r=10.0, G_m =4.0, M=0.5, R=0.2, S_r= 1.0, S_c= 0.6, D_f= 0.2, K= 0.5.

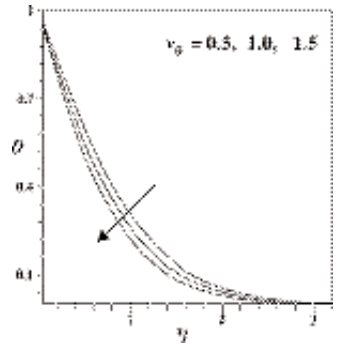

Fig. 18. Temperature profiles for different values of v_o with G_r=10.0, G_m=4.0, M=0.5, R=0.2, P_r= 0.71, S_r= 1.0, S_c = 0.6, D_f= 0.2, K= 0.5.

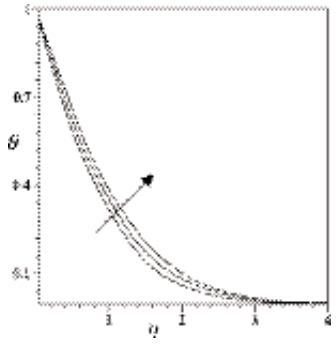

Fig. 19. Temperature profiles for different values of D_f with v_o=0.5, G_r=10.0, G_m=4.0, M=0.5, R=0.2, P_r= 0.71, S_r= 1.0, S_c = 0.6, K= 0.5.

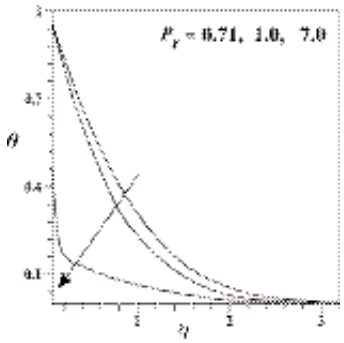

Fig. 20. Temperature profiles for different values of P_r with v_o =0.5, G_r=10.0, G_m=4.0, M=0.5, R=0.2, S_r= 1.0, S_c = 0.6, D_f= 0.2, K= 0.5.

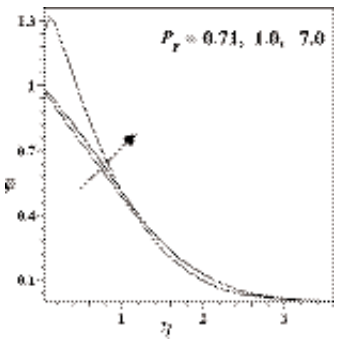

Fig. 23. Concentration velocity profiles for different values of P_r with v_o=0.5, G_r=10.0, G_m =4.0, M=0.5, R=0.2, S_r= 1.0, S_c= 0.6, D_f= 0.2, K= 0.5.

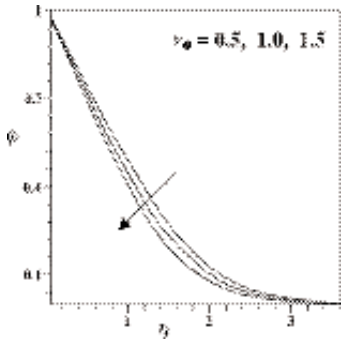

Fig. 21. Concentration profiles for different values of v_o with G_r=10.0, G_m =4.0, M=0.5, R=0.2, P_r= 0.71, S_r= 1.0, S_c= 0.6, D_f= 0.2, K= 0.5.

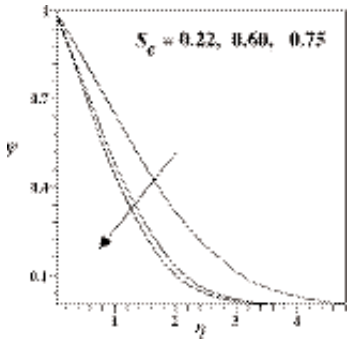

Fig. 24. Concentration profiles for different values of S_c with v_o=0.5, G_r=10.0, G_m =4.0, M=0.5, R=0.2, P_r= 0.71, S_r= 0.71, D_f= 0.2, K= 0.5.

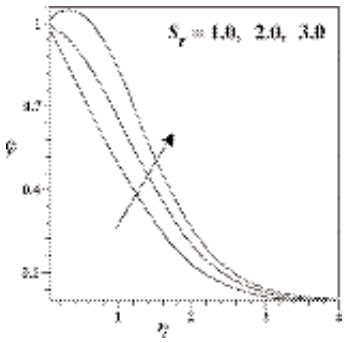

Fig. 22. Concentration profiles for different values of S_r with v_o=0.5, G_r=10.0, G_m =4.0, M=0.5, R=0.2, P_r= 0.71, S_c= 0.6, D_f= 0.2, K= 0.5.

observed from this figure that the Soret number (S_r) has a large increasing effect on concentration. In Fig. 23 and 24, the effects of Prandtl number (P_r) and Schmidt number (S_c) on the concentration field are shown respectively. It is observed from these figures that the concentration increases as the Prandtl number (P_r) increase. It is also seen from these figures that the Schmidt number (S_c) has a major decreasing effect on the concentration field.

Finally, the effects of various parameters on the components of skin-friction (τ_x and τ_z), the Nusselt number (N_u) and the Sherwood number (S_h) are shown in Tables I-III.

From Table I, we observe that the skin-friction component (τ_x) decreases while the skin-friction component (τ_z), the Nusselt number (N_u) and the Sherwood number (S_h) increase with the increase of the suction parameter (v_0). It is also seen from this table that the skin-friction component (τ_x) and the Nusselt number (N_u) decrease while the skin-friction component (τ_z) and the Sherwood number (S_h) increase with the increase of magnetic parameter (M).

Again, from Table II, we see that the skin-friction components (τ_x and τ_z) decrease with the increase of rotation parameter (R), but the Nusselt number (N_u) and the Sherwood number (S_h) increase with the increase of rotation parameter (R). It is also seen from this table that the skin-friction component (τ_x) and the Nusselt number (N_u) increase with the increase of Soret number (S_r), but the skin-friction component (τ_z) and the Sherwood number (S_h) decrease owing to the increase of Soret number (S_r). Also, from Table III, we observe that the skin-friction component (τ_x) and the Sherwood number (S_h) increase with the increase of Dufour number (D_f), but the skin-friction component (τ_z) and the Nusselt number (N_u) decrease with the increase of Dufour number (D_f). It is also seen from this table that the skin-friction component (τ_x) and the Nusselt number (N_u) decrease while the skin-friction component (τ_z) and the Sherwood number (S_h) increase with the increase of permeability parameter (K).

References

Anghel, M., Takhur, H.S. Pop, I. (2000): Dufour and Soret effects on free convection boundary-layer over a vertical surface embedded in a porous medium, Studia Universitatis Babes-Bolyai. *Mathematica*, **XLV(4):** 11.

Alam, M.S. Rahman, M.M. (2006) Dufour and Soret effects on mixed convection flow past a vertical porous flat plate with variable suction, *Nonlinear analysis: Modeling and Control*, **11:** 1.

Debnath, L. (1975) Inertial oscillations and hydromagnetic multiple boundary layers in a rotating fluid, *ZAMM*, **55:** 141.

Debnath, L., Roy, S.C. Chatterjee, A.K. (1979) Effects of hall current on unsteady hydromagnetic flow past a porous plate in a rotating fluid system, *ZAMM*, **59:** 469.

Eckert, E.R.G. Drake, R.M. (1972) Analysis of Heat and Mass Transfer, McGraw-Hill Book Co., New York.

Georgantopoulos, G.A. (1979) Effects of free convection on the hydromagnetic accelerated flow past a vertical porous limiting surface, *Astrophysics and Space Science*, **65:** 433.

Gebhart, B. Pera, L. (1971) The nature of vertical convection flows resulting from combined buoyancy effects of the thermal and mass diffusion nature, *Interrnational Journal of Heat and Mass Transfer,* **14:** 2025.

Kafoussias, N.G. Williams, E.M. (1995) Thermal-diffusion and diffusion-thermo effects on mixed free-forced convective and mass transfer boundary layer flow with temperature dependent viscosity, *Internatinal Journal of Engineering Science,* **33:** 1369.

Nanousis, N., Georgantopoulos, G.A. Papaioannou, A. (1980) Hydromagnetic free convection flow in the stokes problem for a porous vertical limiting surface with constant suction, *Astrophysics and Space Science,* **70:** 377.

Na, T.Y. (1979) Computational Method in Engineering Boundary Value Problem, Academic Press, New York.

Pai, S.I. (1962) Magnetogasdynamics and Plasma dynamics, Springier Verlag, New York.

Raptis, A. Singh, A.K. (1983) MHD free convection flow past an accelerated vertical plate, *International Communications in Heat and Mass Transfer,* **10:** 313.

Raptis, A. Singh, A.K. (1985) Rotation effects on MHD free convection flow past an accelerated vertical plate, *Mechanical Resulation Communication,* **12:** 31.

Rapits, A.A Perdikis, C.P. (1982) Effects of mass transfer and free-convection currents on the flow past an infinite porous plate in a rotating fluid, *Astrophysics and Space Science*, **84:** 457.

Singh, A.K. (1982) MHD free convection flow in the stokes problem for a porous vertical plate, *Astrophysics and Space Science,* **87:** 455.

Singh, A.K. (1984) Hydromagnetic free convection flow past an impulsively started vertical plate in a rotating system, *International Communications in Heat and Mass Transfer*, **11:** 349.

Singh, A.K. Singh, J.N. (1989) Transient MHD free convection in a rotating system, *Astrophysics and Space Science*, **162:** 85.

Sattar, M.A. Alam, M.M. (1994) Thermal diffusion as well as transpiration effects on MHD free convection and mass transfer flow past an accelerated vertical porous plate, *Indian Journal of Pure and Applied Mathematics*, **25:** 679.

Schlichting, H. (1968) Boundary Layer theory, McGraw-Hill, New York.

Received : April, 22, 2007;
Accepted : September, 11, 2007